The **Biophysicist**

A Homebuilt Experiment to Quantify the Mechanical Properties of Hair

Fabian Bennati Weis^{1,§}, Tizian Schmidt^{1,§}, Kilian Kuhlbrodt^{1,§}, Ruth Meyer¹, Charlotta Lorenz^{1,2,*}, Sarah Köster⁰^{1,*}

ABSTRACT Gaining research experience early on is instrumental for undergraduate students, motivating them and improving their comprehension of science. Here, we present an experimental setup that does not require access to state-of-the-art research laboratories and that provides hands-on conceptual and experimental insights into biophysical research. Due to time constraints, such research-oriented hands-on skills are commonly less in focus during undergraduate studies. With our experiment, students can simultaneously record force-strain curves and measure the diameter of micrometer-diameter fibers (such as hair) to examine elongation, stiffness, dissipated energy, and the Poisson ratio. To study these properties, the students familiarize themselves with different data analysis tools, including image processing and data fitting, and compare the results to those in the literature. The data analysis includes challenges typical for biophysics such as sample-to-sample variations, signal fluctuations, and a limited number of available samples. The students accompany the entire process of experimental development, analysis, interpretation, and discussion of data. We furthermore provide instructions and code for automating the experiment. Our experiment thus narrows the gap between didactic aims and current practice in undergraduate experimental courses in biophysics.

KEY WORDS mechanics; optics; force–strain measurements; hair; interference; homebuilt; undergraduate

I. INTRODUCTION

Life relies on the mechanical stability and resilience of biological organisms and their components (1). Failure of mechanical stability can result in diseases (2, 3). For example, mutations in the keratin 5/14 system can cause fragile skin with blisters and injuries upon mechanical stress (4). Disturbed mechanical signaling cascades promote cancer growth (5). Thus, it is of great importance to study the mechanical properties of biological systems. Biological physics offers a toolbox to understand and quantify biomechanics.

Nowadays, biophysics lectures and laboratory courses are offered in undergraduate physics studies. However, even under optimal circumstances (e.g., well-prepared students working in a laboratory with state-of-the-art research equipment), it may be challenging to directly transfer the students' theoretical knowledge from lectures to real science experiments, mostly due to time restrictions during educational programs. Specifically, biophysics experiments are challenging due to high interdisciplinarity, noise from thermal fluctuations as common in biological samples, sample-to-sample variations, and a limited number of experiments or studied samples.

Received: 4 September 2024 Accepted: 8 January 2025 Published: 11 April 2025

© 2025 Biophysical Society.

¹Institute for X-Ray Physics, University of Göttingen, Göttingen, Germany ²Department of Materials Science and Engineering, Cornell University, Ithaca, NY, USA

[&]quot;*" corresponding authors

[&]quot;§" equal contribution

To bridge the gap between classical undergraduate education (i.e., lectures and lab courses) and biophysics research, we report an example of a student project from conceptualization to data analysis, interpretation, and publication. Three undergraduate students, the 3 co-first authors of the paper, performed the research under the supervision of the 3 remaining authors. Although we present our concept on a very concrete example—the mechanical study of hair—we believe it can be generalized to other examples from biophysics and beyond.

The setup is completely homebuilt, offering students a large degree of independence and ensuring low overall costs for the setup. Building and comprehending the setup fosters understanding of elasticity theory, basic electronics, and wave optics (i.e., constructive and destructive interference), so a broad range of undergraduate physics topics is covered. The biological sample for these studies is hair, which is mechanically interesting due to its complex structure and easy accessibility. Our choice of biological system and quantities measured poses challenges that are typical for biophysics.

II. SCIENTIFIC AND PEDAGOGIC BACKGROUND

A. Scientific background

A central goal of biophysics is to understand the behavior of complex, biological systems by applying the methods and fundamental laws of physics. Biology includes many interesting and complex mechanical phenomena that are studied within this framework. Such studies shed light on the function and structure of biological samples. We suggest that in preparation of such projects, undergraduate students read about fundamental continuum mechanics concepts in standard mechanics textbooks (6–8).

Important mechanical parameters are the stiffness, the elongation upon loading (the stress–strain response), and the viscoelastic behavior (the amount of energy stored or dissipated during mechanical deformation). The mechanical response of one-dimensional materials

to a small deformation Δx is described by Hooke's law. The force driving the system back to its equilibrium position is related to the linear deformation via the spring constant k:

$$F = -k\Delta x \tag{1}$$

Consequently, for large or small values of k, a high or low force, respectively, is required to cause a specific displacement. When deforming the system against this force, the amount of work W performed along a path $\vec{x}_1 \rightarrow \vec{x}_2$ is given by

$$W = \int_{\vec{x}_1}^{\vec{x}_2} \vec{F(\vec{x})} d\vec{x}$$
 (2)

This quantity generally depends on the exact path of the system and the velocity along the path. Considering a closed loop $\vec{x}_1 \rightarrow \vec{x}_2 \rightarrow \vec{x}_1$, the system exhibits hysteresis if the response of the system along the extension path $\vec{x}_1 \rightarrow \vec{x}_2$ is different from the response along the relaxation path $\vec{x}_2 \rightarrow \vec{x}_1$. If the total work over the closed path is positive, energy has been dissipated by the system. The dissipated energy can be an important indicator for internal processes such as structural transformations.

The structural transformation may be associated with a change in the length, width, or height of the object. The extension normalized to the length L_0 , or strain $\varepsilon = \Delta x/L_0$, renders data from different samples comparable to one another. Correlated changes in an object's width, height, and length can then be described with the Poisson ratio v

$$v = -\frac{\varepsilon_z}{\varepsilon_r} \tag{3}$$

where ε_z is the strain in the direction of stretching and ε_r the strain in the axial direction. If the strained object is a thin, long fiber, the former can be measured just by a ruler and controlled by a step motor. In contrast, the resulting axial strain may be too small to be measured by the same techniques. Instead, optical measurements using the coherence properties of laser light in diffraction experiments can be used to determine the width of a sample.

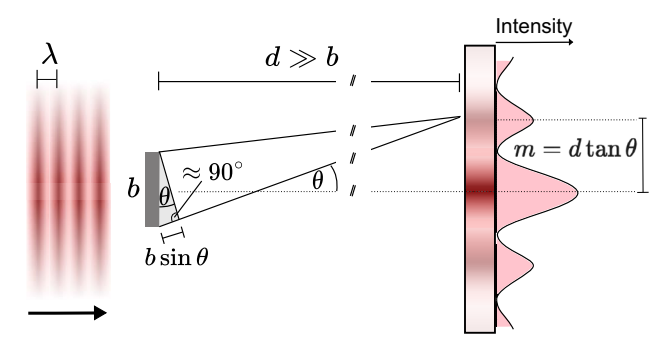


Fig 1. Schematic view of the diffraction of monochromatic, coherent light represented by red light waves coming from the left. The light is diffracted from a small object of diameter b at an angle θ to the incoming beam. The diffraction pattern is observed on a screen at distance $d \gg b$. The nth maximum of light intensity on the screen is observed if $b\sin\theta = \pm n\lambda$, and it appears on the screen at a vertical distance $m = d\tan\theta$ from the central maximum. During the measurements, the distances d and m are determined. From these parameters, b is calculated as $b = \pm n\lambda/\sin(\tan^{-1}(m/d))$.

Diffraction of coherent light from an object with size b depends on the wavelength of the light λ . If $b \ll \lambda$, diffraction effects are minimal, making the object appear as a point source and thus limiting size determination. If $b \gtrsim \lambda$, clear diffraction patterns can be observed on a screen at a distance d far away from the object, allowing for precise size measurements. Finally, if $b \gg \lambda$, diffraction effects are negligible, and the object's shadow can be observed without detailed patterns. However, thickness measurements for $b \gg \lambda$ can be precisely carried out with other measurement techniques such as light microscopy. A sketch of a diffraction experiment is shown in Figure 1, and the procedure to calculate the object's thickness b from the positions of the interference maxima is explained in the caption. With this diffraction measurement, we measure the thickness of hair and its change in diameter upon stretching.

Hair is a biological material with very intriguing mechanical properties. It is also well suited for undergraduate student experiments, because it is macroscopic, extensible, and available for low cost in sufficiently large amounts. Despite the great variety of mammalian species and different hair types, all mammalian hair shows a similar mesoscopic structure. It can generally be divided into 3 different components: cuticula, cortex, and medulla; see

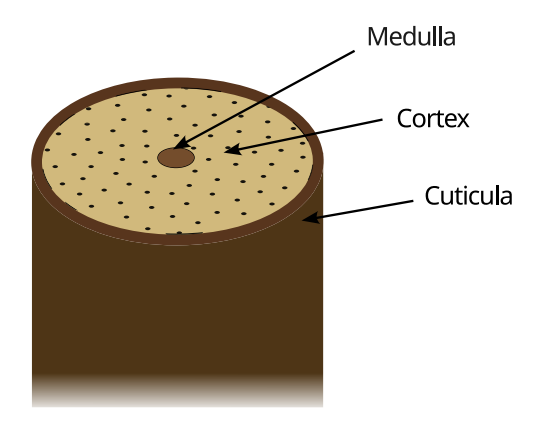


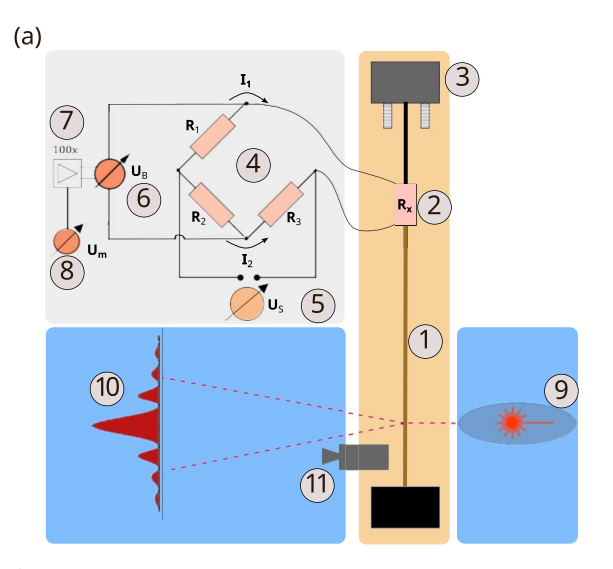
Fig 2. Schematic of the cross section of mammalian hair, representing its internal structure, consisting of 3 major parts. The medulla forms the core of the hair and is embedded in the cortex. The outermost part is the cuticula, a harder, thinner layer that protects the softer internal structures (9).

Figure 2 (9). The cuticula forms the outermost layers and is composed of dead flattened cells whose dominant component is cytoskeletal keratin, crosslinked by high numbers of disulfide bonds. The cortex is the predominant structure in hair and consists of dead elongated cells. The main components of the cortical cells are type I and II keratins and keratin-associated proteins (10). The medulla is located in the center of the hair and consists of dead cells and air. The dead cells contain mostly epithelial and hair keratins (11).

B. Pedagogic background

Mechanics is typically one of the first topics high school and undergraduate students are exposed to during physics studies. This is for good reason, because the topic can intuitively be connected to daily life experiences. However, applying the underlying physical principles to experiments often includes some challenges, specifically in biophysical experiments.

Although students typically know which parameters need to be measured to describe a system from a mechanical standpoint, the actual implementation of the measurement can be challenging. For example, parameters such as the spring constant are not directly accessible but need to be measured via other parameters such as the force required to extend the system by a certain amount. Thus, the determination of the spring



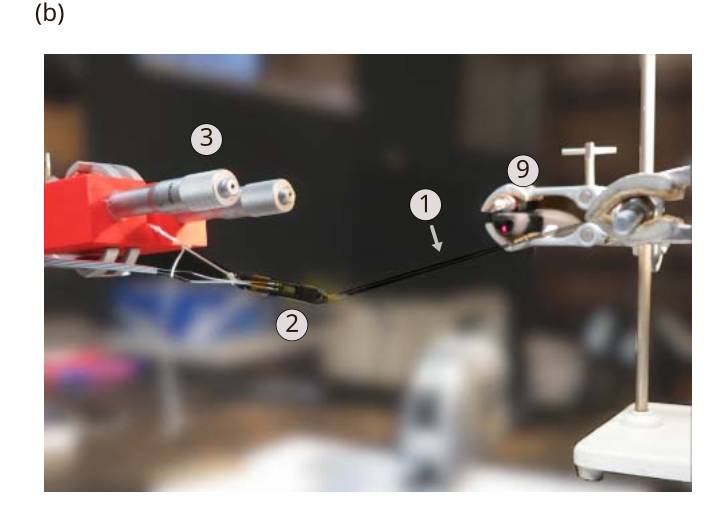


Fig 3. (a) Schematic view of the experimental setup, which consists of a stretcher (orange), electronics (gray) to record signals from the strain gauge, and an optic interference measurement (blue). The numbers (no.) indicate the following: the hair to be investigated (no. 1); the strain gauge (no. 2); screws to adjust the extension (no. 3); a bridge circuit (no. 4); the source voltage of the bridge circuit (no. 5); the bridge voltage (no. 6); the input of the amplifier (no. 7); the output voltage of the amplifier (no. 8); the laser (no. 9) pointing toward the screen on which the interference pattern is recorded (no. 10); and the camera recording the interference pattern (no. 11). (b) Photograph of the stretcher including the hair (no. 1), the strain gauge (no. 2), extension screws (no. 3), and the laser pointer (no. 9).

constant is more sophisticated than one may expect.

Biological systems typically consist of many interacting components so that small changes of the components and, thus, changes in interactions, can lead to measurable differences between samples. Therefore, variations between samples may be larger than in macroscopic samples studied by students in laboratory courses beforehand. Consequently, in the project described here, students learn to analyze and interpret data that include more variation and noise than found in samples they studied so far. The analysis requires a considerable amount of numerical analysis and image processing, which is not necessarily taught in typical undergraduate courses.

III. MATERIALS AND METHODS

A. Experimental setup

The experimental setup is shown schematically in Figure 3a, and a photograph of the setup during a measurement is displayed in Figure 3b. The setup consists of 3 main elements: the stretching apparatus (orange-shaded area), a part containing electronics to convert the force acting on the hair

into an electronic signal (light gray), and an interference experiment (blue) to measure the hair's thickness. A detailed list of the components can be found in the Supplemental Material. The hair (no. 1) is attached to a fixed mount on one side and to a strain gauge platelet on the other side. The strain gauge (no. 2) measures the force applied to the hair. The strain gauge is supported by an elastic 3-dimensional (3D)-printed platelet that is connected to an extension stage. The stage consists of a 3D printed box cart that is positioned inside the box with micrometer screws (no. 3). These screws control the strain of the hair. In the Supplemental Material, we provide computer-aided design files for 3D printing of these parts. The strain gauge (no. 2) is a sensor made of a wound conductor that changes its electrical resistance proportionally to the strain applied to it. It can thus be regarded as a strain-sensitive resistor. To measure these small changes in resistance, a Wheatstone bridge (no. 4) is used, as shown in Figure 3a, with a controlled source voltage U_S (no. 5) and known resistors $R_1=R_2=100~\Omega$ and $R_3=350~\Omega$. In this configuration, if $R_1/R_x = R_2/R_3$, the bridge is balanced ($U_B = 0 \text{ V}$), and any change in R_x leads

to a proportional change in the measured bridge voltage U_B (no. 6). Because these changes are small, the bridge voltage is amplified 100-fold (no. 7) to obtain the measured voltage U_m (no. 8). This circuit thus provides a linear relation between the measured voltage U_m and the strain on the hair, which can be calibrated with known weights. Note that the strain-free resistance $R_x = R_3$ is chosen, so the changes in thermal resistance due to current heating do not affect the bridge voltage.

To measure the thickness of the hair, a standard laser pointer (wavelength 650 nm, power < 1 mW; no. 9) is directed toward the hair, so the diffraction pattern is visible on a screen or wall (no. 10), with the hair as the diffracting object. This pattern is recorded with a camera (no. 11) and can be used to determine the width of the hair. Although a standard, commercially available laser pointer is used, students should be aware of the risks and necessary precautions for its use.

B. Measurements

In our experimental design, the force F acting on a stretched material is proportional to the measured voltage over the Wheatstone bridge $U_{\rm B}$ (Fig 3a). To determine the proportionality factor between the weight and the voltage, the setup is calibrated before each set of measurements with weights that exert forces from 0 to 3.5 N.

As samples, tail hair from the same horse is used in all measurements. Although human hair may be considered the first choice, horse hair can withstand greater forces and longer extensions, while showing similar mechanical behavior. It, therefore, better matches the characteristics of our setup, especially the strain increments and precision attainable with the micrometer screws, and thus facilitates the acquisition and improves the quality of the measured data.

In the general stretching procedure, the hair is tethered between 2 mechanical clamps at equal heights. The clamps are moved apart until the hair becomes nearly straight. The hair is not pulled into a fully straight position to ensure that the measurements begin in a regime without strain, so the full force–strain

curve is recorded, and prestress, leading to hysteresis, is avoided. From this extension on, the additional extension of the hair is measured. We increase the elongation in 1-mm steps to a maximum of 25 mm and subsequently decrease it with the same step size. Between each step, the force is measured after holding the strain constant for 6–10 s. Upon stretching the hair up to a length of L, we define the strain $\varepsilon = (L/L_0) - 1$, where L_0 corresponds to a strain of 0, to quantify the elongation relative to its rest length. The stretching procedure is repeated 3 times consecutively for each sample.

In this manner, we investigate the behavior of 6 dry hairs and 6 wet hairs to compare the dependence of the elastic behavior in the 2 most frequent media (12). We were able to stretch some hair for more than 10 cycles. For the wet hair, the fixations of the hair are repositioned, so most of the hair is submerged in a water reservoir, while the end stripped to the strain gauge is kept dry to protect the electronics. For 2 samples, we record interference patterns in 1-mm steps to monitor the thickness during a stretching cycle.

IV. RESULTS

To quantify the mechanical properties of hair, we measure its force-strain behavior. Typical stretching and relaxation curves are shown in Fig. 4 (top), starting with the first stretching and relaxation cycle, represented in bright green. Darker colors represent consecutive cycles. We observe hysteresis: the relaxation curve does not follow the stretching curve. The form of consecutive cycles changes, as we stretch and relax repeatedly, and the area between the stretching and relaxation cycle decreases. Interestingly, for measurements of hair submerged in water, the curves for consecutive cycles look similar, indicating no significant permanent modifications of the hair (Fig 4, bottom). Yet, stretching and relaxation still differ, indicating that energy is dissipated in an aqueous environment as well, albeit less than for dry hair.

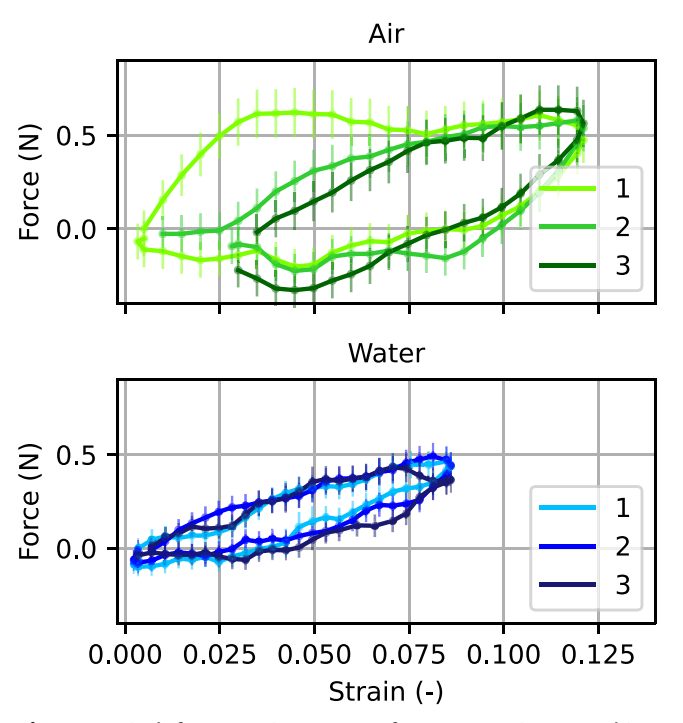


Fig 4. Typical force—strain curves of 3 consecutive stretching cycles of hair in both air (green, top; dry hair) and water (blue, bottom; wet hair) environments. The hair in air exhibits signs of inelastic stretching, whereas the hair stretched in water suggests mostly elastic behavior. Each force is measured relative to the start of the first cycle. Error bars represent voltage fluctuations during the measurement process based on the largest and smallest measured voltage at a given strain. The line lies between these fluctuations. The measurement and its error bars are converted to the applied force through the calibration measurement described in section III.B. A moving average taking into account 3 measurement points is applied to reduce statistical fluctuations, and the resulting error bars have been calculated accordingly. Further discussion of the moving average is in the Supplemental Material.

A. Stiffness

To characterize the linear mechanical response to an applied strain, we measure the stiffness of the hair. It can be approximated in our data by fitting a line to the force—strain curve (Fig 5a). In this context, the question arises of how to select the appropriate set of data points for the fit. We first manually choose a strain value we are confident in from the appearance of the curve to determine that it is within the linear regime. We then fit a line to the data for a range of at least 3 strain values around this central point. We vary the number of data points included in the fit to find the range of strains with the

smallest fit errors and select this fit to represent the stiffness.

To compare the stiffness of dry hair after repeated loading, we normalize the stiffness for each extension to the stiffness at the beginning of the first cycle, ranging between 90 and 240 N/m in our samples. The normalized stiffnesses are shown in Figure 5b. On average, dry hair softens by ~50%. For wet hair, we generally observe a lower stiffness by comparing the force-strain curves (see Fig. 4). The softer behavior of wet hair and thus higher relative noise levels make it difficult to analyze the stiffness with the same procedure that we use for dry hair. Comparing the shape and magnitude of the force-strain curves of wet and dry hair, nonetheless, leads us to the conclusion that wet hair is softer than dry hair and that wet hair does not soften significantly during repeated loading up to strains of 0.08.

B. Elongation

Because we observe a change in stiffness of 50% upon repeated stretching of dry hair, the question arises of whether the hair undergoes structural changes and plastic deformation when stretched. One could expect that such a drastic change in stiffness is due to a change in diameter and in length of the hair because a thinner and more elongated hair could be softer. Thus, we examine the hair for permanent deformation. Specifically, we quantify the residual length of the hair after stretching. We analyze the elongation by extending the method used to determine the stiffness: In addition to the linear fit for low strains, we find a linear approximation of the force-strain curve near the point where the hair hangs loosely again during relaxation (see gray line in Fig 5a). The linear fits during extension and retraction intersect at a finite strain value that we call the *neutral point*. From the difference between this strain value and the neutral point of the previous cycle, we infer the elongation of the hair after each cycle. The calculated elongations of 6 samples of horse hair stretched in air are shown in Figure 5c. All samples exhibit an elongation. On average, the hair samples elongate by

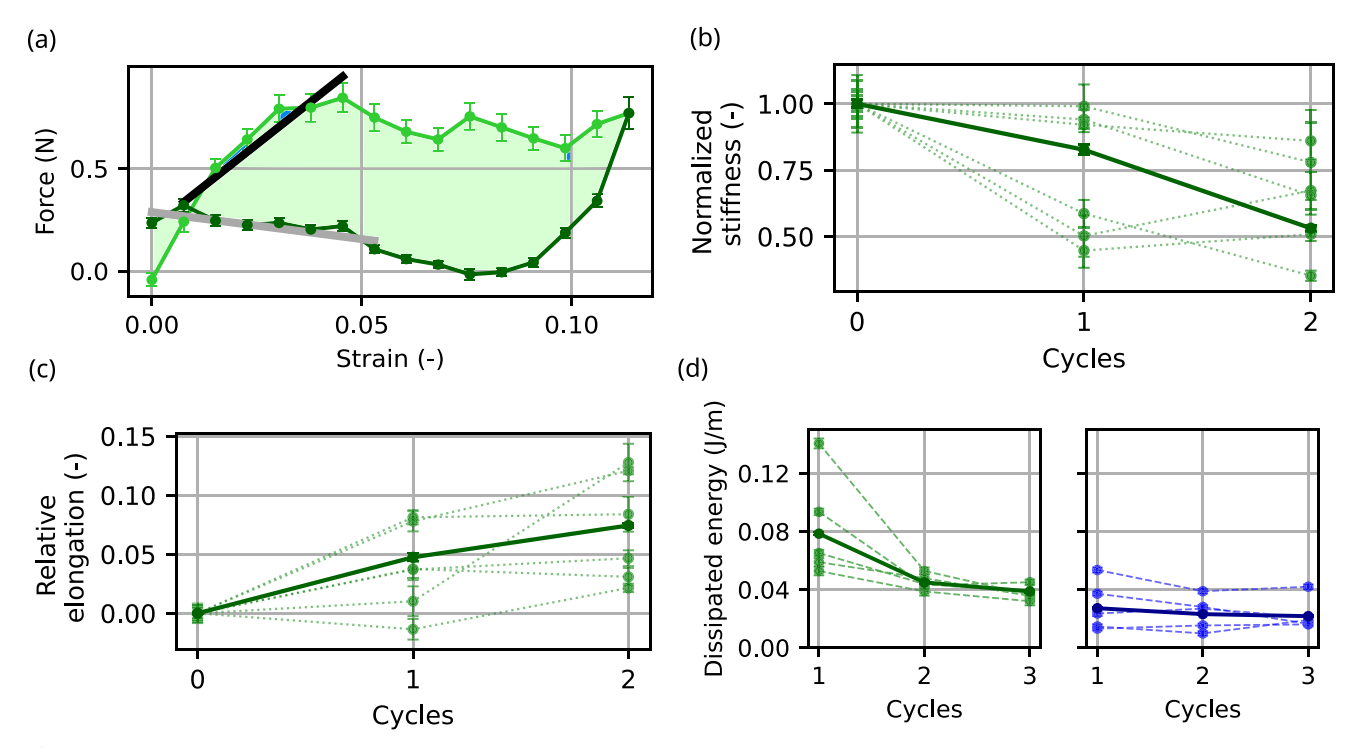


Fig 5. (a) A typical force—strain curve of a hair. The green area in between the curves corresponds to the total dissipated energy per unit length of the hair for one cycle. The black and gray lines show linear fits, as described in the text. (b) Normalized stiffness across 2 extension cycles in air for 6 hair samples. The repeated stretching results in decreasing stiffness. The dotted lines represent individual samples and the solid lines the weighted mean across all hair samples for each cycle. (c) Relative elongation compared with the initial length across 2 cycles for 6 hair samples. The repeated stretching leads to increasing elongation. (d) Dissipated energy per hair length during cyclic stretching of hair in air (green) and in water (blue). Although the dissipated energy of hair in air decreases during 2 cycles, hair dissipates the same energy during several stretching cycles. This dissipated energy of hair stretched in water is lower than the dissipated energy of hair stretched in air.

7.5% after 2 cycles, with maximum strains between 0.12 and 0.17.

C. Energy dissipation

As shown in Figure 5a, the hair does not only elongate, but also energy is dissipated. This dissipated energy could indicate structural changes within the hair. To understand better how this structural change could occur, we analyze the dissipated energy during each stretching and relaxation cycle. We find a pronounced memory effect of the dissipated energy per hair length of stretched dry hair: the weighted mean of the energy dissipated by the hair decreases from 0.08 J/m in the first cycle to 0.04 J/m in the third cycle (Fig 5d, left panel). This tendency is observed for all measurements and indicates that bonds within the filament are broken and do not reform during the relaxation cycle. These broken bonds may lead

to the elongation of the hair. Interestingly, if hair is stretched in water (Fig 5d, right panel), the dissipated energy is very similar throughout all cycles. One possible explanation on the microscopic level could be that bonds break as well during extension, but the filaments are able to "slip back," restoring the bonds. The ability to reform bonds would also explain why the extension and retraction curves in water have similar appearances (Fig 4). An alternative explanation of different behavior of dry and wet hair could be the absence of specific bonds in water because hair in water appears softer during the first cycle.

D. Thinning and the Poisson ratio

Because the hair elongates upon stretching, a concomitant thinning of the hair may be expected. Therefore, we measure the hair's diameter during stretching and relaxation with

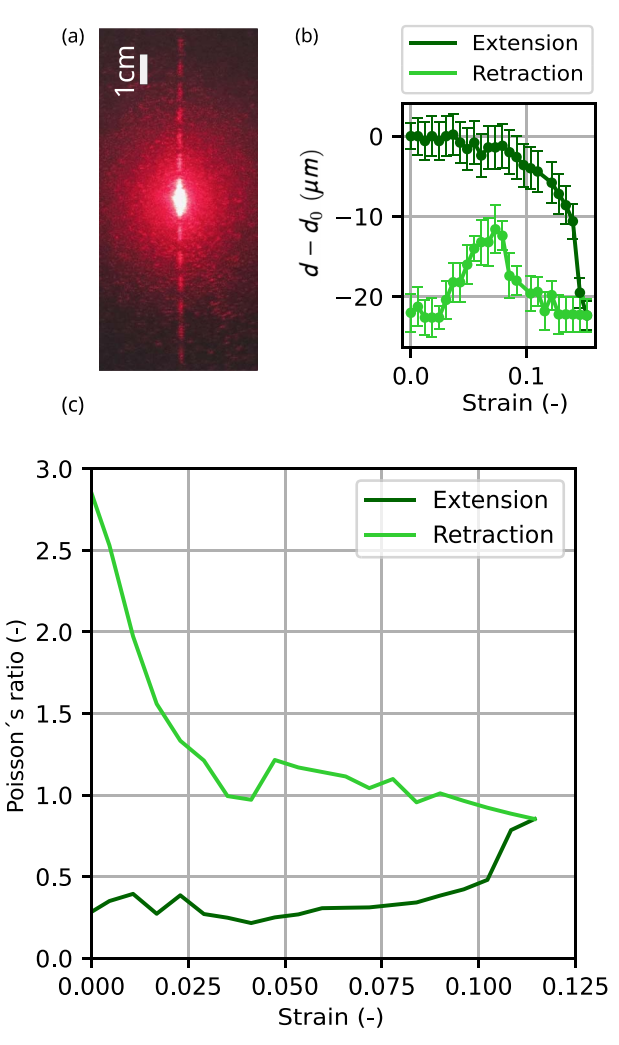


Fig 6. (a) Typical image of the resulting interference pattern of laser light diffracted by hair used for the calculation of the diameter of the hair. (b) Plot of the absolute difference $d-d_0$ in hair diameter with respect to the diameter at zero strain against the applied strain. At low strains, we observe little change, whereas for higher strains, the diameter decreases rapidly. These high strains lead to a nonreversible reduction in hair diameter. Upon relaxation, there is an initial increase in diameter, after which the diameter returns to the diameter under maximum applied strain. We believe that the initial increase is not a real physical feature of the system, but rather a measurement artifact, because at zero strain, we again observe the same diameter as under maximum applied strain. (c) The diameter change is used to calculate the Poisson ratio during the repeated stretching. In the low-strain regime, the Poisson ratio stays approximately the same, with a mean of 0.44 \pm 0.12. The Poisson ratio increases above strains of 0.1 and does not decrease under relaxation, indicating a nonreversible structural change. For the retraction, we observe a strong increase in the Poisson ratio. This increase is not a physical feature of the system, because the Poisson ratio is not well defined for the retraction anymore, due to the permanently changed diameter under zero strain.

the diffraction of laser light for a measurement in air (Fig 6a). The measurement cannot be done in water because the hair is submerged inside of water in a container. The interference pattern after passing through the container is not exact enough for a measurement. We observe a significant decrease in the diameter for strains above 0.1 (Fig 6b). When we decrease the strain after the extension period, we first observe an increase in the diameter and a subsequent decrease. We consider the initial increase in the diameter upon retraction to be a measurement artifact. A possible reason could be nonhorizontal alignment of the hair during the measurements. We do not expect this increase to be a real feature, because under zero strain, the hair does not regain its original diameter, returning to the diameter under maximum strain. This leads us to the assumption that the hair has permanently thinned. This assumption is supported by the rapid decrease in the difference in diameter at strains above 0.1. It indicates that we are above the yield point, exceeding the reversible deformation region, where further extensions begin to deform the hair irreversibly (13). Permanent thinning of the hair also indicates nonreversible changes in the molecular structure of the hair. To combine the thinning and elongation of the hair in one parameter, we calculate the Poisson ratio (Fig 6c). Note that the Poisson ratio is well defined only for reversible systems. The ratio is limited by $-1 \ge v \ge 0.5$ (14). Figure 6c shows that an irreversible process for strains above 0.1 takes place. Therefore, we calculate the Poisson ratio for the elastic region by calculating the mean value for strains under 0.1. In this region, the mean (\pm SD) Poisson ratio is calculated to be 0.44 \pm 0.12, which agrees with the results of Hu et al., who found a Poisson ratio of 0.377 (15). For strain values above 0.1, the Poisson ratio increases above 0.7 in the extension region and further increases during the retraction period to almost 3. This indicates that we are outside of the elastic stretching region, again substantiating the hypothesis that a permanent structural change has occurred.

V. DISCUSSION

A. Scientific discussion

We built a setup that can measure the stiffness, elongation, dissipation, and Poisson ratio of hair in air and water without advanced laboratory equipment. For experiments conducted in air, our data agree well with literature: We determine the Poisson ratio of horse hair in air to be 0.44 \pm 0.12. Hu et al. measured a Poisson ratio of 0.377 for human hair in air (15). Another study found that the plateau-like behavior, in which the hair can be further extended without increasing the applied force, in force-strain measurements of stretched hair starts at strains of 0.18 (16), while the plateau for our datasets is at strains of around 0.04. However, because the studies were carried out with hair from different origins (human and horse), the difference probably results from this fact and possibly specific differences in the elements, such as the number of disulfide bridges. Yu et al. also studied the mechanics of human hair in water and reported a reduced stiffness of wet hair with respect to dry ones, as we observed it (17), which the authors explained by the water acting as a plasticizer, reducing the interaction among the proteins. Yet, in their work, the full hysteresis curve is not recorded, so the behavior across multiple stretching cycles additionally reported in the present work cannot be compared with Yu et al. (17).

With our comparatively simple, homebuilt setup, we can conclude that the structure of the stretched hair is plastically deformed, resulting in a notable alteration to its inner structure. Similar conclusions about deformations and structural changes are also drawn from conceptually analogous experiments on the micrometer scale for intermediate filament proteins (18–21). A major component of hair is keratin (see section II), which is a member of the intermediate filament protein family (20, 21). The force–strain behavior we observe is surprisingly similar to the behavior of the micrometer-sized filaments, yet the structures of hair and the micrometer-sized filaments are

very different, so a direct comparison would not be reasonable.

B. Pedagogic discussion

With the homebuilt setup introduced here, students can accompany the process from designing a setup and an experiment to data acquisition, analysis, and discussion. In our case, the students were included in the manuscript writing and publication process. With all these steps, students experience the entire scientific process and are well prepared for transferring the skills they acquired in lectures to experiments. In the case presented here, the students handled these challenges very well with advice from technicians and scientists. The experience the students obtained during the project helped them to conduct further state-of-the-art experiments in biophysics and other areas of physics. To give an example of acquired and transferable skills, the students explored different strategies to handle the noise and realized that a smoothing average led to the most reasonable and stable results. The students also had to apply averaging procedures during image analysis, a new skill they acquired during the project.

The entire project, including the building of the setup and a written report, took the equivalent of ~1 month in total, assuming full-time work. In our case, the students worked on the setup part time, ~1 working day per week. If the setup is already assembled, several measurements can be conducted within a day. Depending on the number of workdays per week and progress, regular meetings with the supervisors support the success of the project. In our case, the supervisors were always available for questions and advice during the experimental days, and more formal supervision meetings and progress reports took place every 2–4 weeks.

A reduced version of the entire project (e.g., without the publication process) may also be suitable for teaching at a high school level, because the topics of mechanics and light diffraction are also taught at a high school level. Here, the project may introduce working on week- to month-long projects and combining

physics and biology to students already at a young age. In particular, measurements of hair in water with shampoo or other cosmetic hair products may be interesting to increase the connection to daily life questions.

The students planned the experiment to be carried out with human hair; however, human hair typically breaks at strains lower than 0.02. Thus, the students had to adapt the project and switched to horse hair, which they stretched up to a strain of 0.16. Of course, other samples can be tried, and the experiments can also be carried out in larger sample sizes. Automation of the setup beyond the initially planned project allowed the students to take more data on human hair during an outreach event. This was particularly interesting for participants because they could directly observe the mechanical properties of their own hair. Codes for taking these data are included as Supplemental Material.

VI. CONCLUSION

We measure the stiffness, elongation, energy dissipation, and Poisson ratio of hair with a homebuilt setup by repeatedly stretching hair in air and water. We find that dry hair softens and extends upon loading, whereas wet hair retains its stiffness. Similarly, dry hair dissipates energy when relaxed, whereas wet hair barely dissipates energy. The Poisson ratio of dry hair agrees well with literature; however, the Poisson ratio diverges for repeatedly stretched hair, indicating permanent damage. All experiments are carried out by undergraduate students who learn to process, analyze, and write about the experimental data. Typically, this entire process is not part of undergraduate studies. Our setup empowers students to undergo the process. preparing them thoroughly for further laboratory work and the publication process.

SUPPLEMENTAL MATERIAL

All Supplemental Material is available at: https://doi.org/10.35459/tbp.2024.000280.51.

AUTHOR CONTRIBUTIONS

CL and SK conceived the project; FBW, TS, and KK carried out the experiments and analyzed the data; CL, RM, and SK supervised the project; and all authors wrote and edited the manuscript.

ACKNOWLEDGMENTS

We thank Peter Luley and the workshop of the Physics Department of the University of Göttingen for technical support. We thank the Faculty of Physics of the University of Göttingen, in particular, Jörn Große-Knetter, Yvonne Lips, and Martin Wenderoth, for the opportunity to perform this "project lab course." Furthermore, we thank Anna Blob, Magdalena Haaf, Kaan Ürgüp, and Jan Goeman for support during the experimental demonstration at the "Night of Science" at the University of Göttingen. The work was financially supported by the European Research Council (grant CoG 724932), the Studienstiftung des deutschen Volkes e.V., and the German Research Foundation (project 523842861, LO3088/1, and project 430255655-KO3572-8/1). We acknowledge support by the Open Access Publication Funds of the University of Göttingen. The authors declare no competing interests.

REFERENCES

- Egan, P., R. Sinko, P. R. LeDuc, and S. Keten. 2015. The role of mechanics in biological and bio-inspired systems. *Nat Commun* 6:7418.
- Zuela-Sopilniak, N., and J. Lammerding. 2022. Can't handle the stress? Mechanobiology and disease. *Trends Mol Med* 28:710–725.
- 3. Di, X., X. Gao, L. Peng, J. Ai, X. Jin, S. Qi, H. Li, K. Wang, and D. Luo. 2023. Cellular mechanotransduction in health and diseases: from molecular mechanism to therapeutic targets. *Signal Transduct Target Ther* 8:282.
- Coulombe, P. A., and C.-H. Lee. 2012. Defining keratin protein function in skin epithelia: epidermolysis bullosa simplex and its aftermath. J Invest Dermatol 132:763

 –775.
- Cooper, J., and F. G. Giancotti. 2019. Integrin signaling in cancer: mechanotransduction, stemness, epithelial plasticity, and therapeutic resistance. *Cancer Cell* 35:347–367.
- Anderson, T. L. 2017. Fracture Mechanics: Fundamentals and Applications. CRC Press, Boca Raton.
- Callister, W. D., Jr, and D. G. Rethwisch. 2020. Materials Science and Engineering: An Introduction. John Wiley & Sons, Hoboken, NJ.
- 8. Hibbeler, R. 2022. Mechanics of Materials. Pearson Education, Boston.
- Bereiter-Hahn, J., A. G. Matoltsy, and K. S. Richards. 1986. Biology of the Integuement: Vertebrates. 1st edition. Springer, Berlin, Germany.
- 10. Robbins, C. 2012. Chemical and Physical Behavior of Human Hair. Springer, Berlin, Germany.
- Langbein, L., H. Yoshida, S. Praetzel-Wunder, D. A. Parry, and J. Schweizer. 2010. The keratins of the human beard hair medulla: the riddle in the middle. *J Invest Dermatol* 130:55–73.
- Wortmann, F., A. Hullmann, and C. Popescu. 2008. Water management of human hair. Int J Cosmet Sci 30:388–389.
- Glaser, R. 2012. Biophysics—An Introduction. 2nd edition. Springer, Heidelberg, Germany.
- Landau, L. D., L. P. Pitaevskii, A. M. Kosevich, and E. M. Lifshitz. 2012.
 Theory of Elasticity. Butterworth-Heinemann, Oxford, UK.
- Hu, Z., G. Li, H. Xie, T. Hua, P. Chen, and F. Huang. 2010. Measurement of Young's modulus and Poisson's ratio of human hair using optical techniques. In Fourth International Conference on Experimental Mechanics. Singapore, 18–20 November 2009. SPIE, Bellingham, WA, pp. 773–781.
- 16. Bull, H. B., and M. Gutmann. 1944. Elasticity of keratin fibers. *J Am Chem Soc* 66:1253–1259.
- Yu, Y., W. Yang, B. Wang, and M. A. Meyers. 2017. Structure and mechanical behavior of human hair. Mater Sci Eng C 73:152–163.
- 18. Block, J., H. Witt, A. Candelli, E. J. G. Peterman, G. J. L. Wuite, A. Janshoff, and S. Köster. 2017. Nonlinear loading-rate-dependent

- force response of individual vimentin intermediate filaments to applied strain. *Phys Rev Lett* 118:048101.
- Block, J., H. Witt, A. Candelli, J. C. Danes, E. J. G. Peterman, G. J. L. Wuite, A. Janshoff, and S. Köster. 2018. Viscoelastic properties of vimentin originate from nonequilibrium conformational changes. Sci Adv 4:eaat1161.
- Lorenz, C., J. Forsting, A. V. Schepers, J. Kraxner, S. Bauch, H. Witt, S. Klumpp, and S. Köster. 2019. Lateral subunit coupling determines intermediate filament mechanics. *Phys Rev Lett* 123:188102.
- C. Lorenz, J. Forsting, R. W. Style, S. Klumpp, and S. Köster. 2023. Keratin filament mechanics and energy dissipation are determined by metal-like plasticity. *Matter* 6:2019–2033.